LOW-REFLECTANCE MATERIAL ON MERCURY: IMPLICATIONS FOR CRUSTAL STRATIGRAPHY AND CARBON DISTRIBUTION FROM REMBRANDT BASIN. L. H. Lark[1], J. W. Head[1], and C. Huber[1], [1]Dept. of Earth, Env. and Planetary Sciences, Brown University, Providence, RI 02912, USA, (laura_lark@brown.edu)

Introduction: Lunar crustal stratigraphy records earliest lunar history and evolution; a primary anorthositic flotation crust separated from the Moon's crystallizing magma ocean, followed by a secondary magmatic crust (mare basalts) that was extruded onto the primary crust [1, 2]. Mercury may have followed a qualitatively similar path. Its magma ocean may have precipitated graphite, which could have floated to form a primary crust [3] which was later buried by voluminous volcanic secondary crust. Impacts formed during and after this period produce exposures of material from which can be derived information about the deep and shallow crustal stratigraphy. This stratigraphy can then be used to place constraints on crustal stratigraphy and the evolution of Mercury's formative years. Ernst et al. [4] explored this for the exposures of low-reflectance material (LRM, possibly darkened by graphite from a primary crust) and high-reflectance red material (HR, interpreted to be of volcanic origin) to understand the stratigraphy of the interior of Caloris basin. They find that the crater exposures are consistent with a volcanic infill origin of the HR and a melt sheet origin of the LRM, giving a minimum thickness of the LRM-bearing layer of 7.5-8.5 km set by its exposure in the central features of Atget. They also noted exposures of LRM associated with Rembrandt and Tolstoj basins but did not undertake a similar analysis to estimate layer thickness and crustal stratigraphy. We extend their methodology to test the hypothesis of a global LRM layer beyond Caloris, then assess implications for Mercury's evolution.

Background: Rembrandt basin (731 km in diameter, located 4000 km from Caloris) has been studied in detail [5, 6, 7]. Crater counts date it as slightly older than Caloris (both ~3.7 Gy), and like Caloris it is associated with units that have been mapped as HR volcanic infill and LRM-bearing impact deposits (ejecta and melt, exterior and interior, including a region of the floor that escaped resurfacing) [6]. The well-preserved nature of the basin and the presence of several large craters intersecting the infilling volcanic plains make Rembrandt an ideal candidate for an extension of the methods of [4] outside Caloris.

Methods: We examine exposures of HR and LRM associated with craters (craters identified by [8], [9], and our own mapping) inside Rembrandt using the Mercury Dual Imaging System false color global mosaic [10] and the maps produced by [7]. We use scaling relationships between crater diameter and maximum excavation and melting depth as summarized by [8] to translate material exposure in ejecta, melt, and central peaks to information about the original location of that material, with the goal of mapping the interface of the HR and LRM and bounding the LRM thickness.

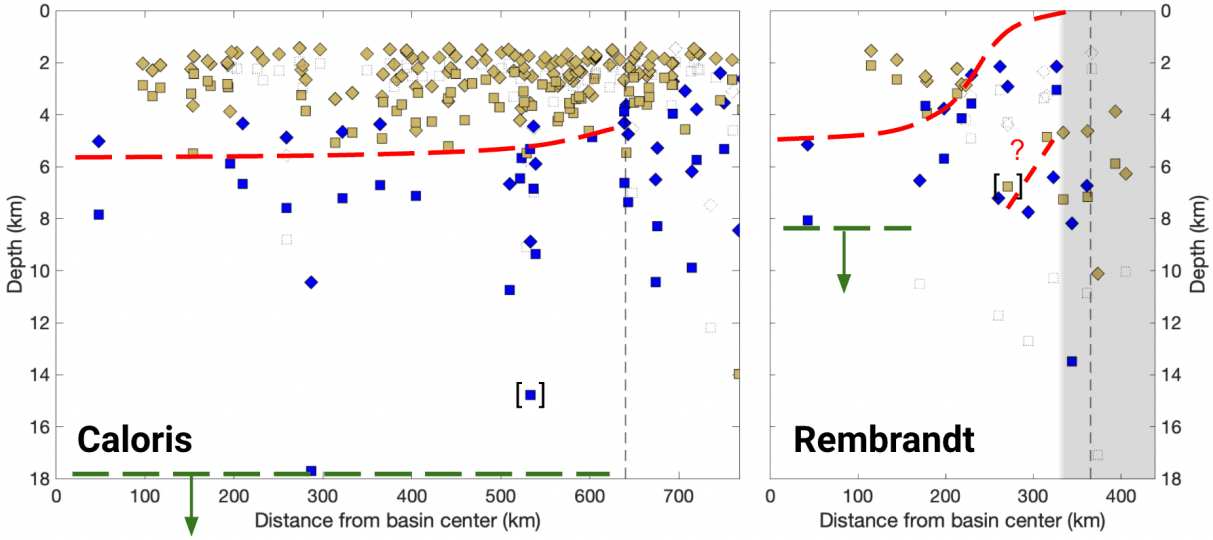

Figure 1. Exposures of red HR (tan markers) and LRM, low-reflectance material (blue markers) by craters in Caloris and Rembrandt basins. On the left are results from [4] for Caloris with depths recalculated to match our methodology for comparison. The right plot shows our results for Rembrandt. Vertical black dashed lines indicate the basin edge; the grey shaded region for Rembrandt indicates craters touching the basin rim. Red dashed lines indicate approximate HR-LRM boundaries; green indicates the shallowest bottom boundary of the LRM.

Results and discussion: Exposures of HR and LRM in Rembrandt basin (Figure 1) are consistent with the presence of a HR volcanic layer ~4 km thick at the basin center (and ~2.5x10^5 km^3 in volume, consistent with other estimates for Rembrandt [7]). This overlies a LRM layer that is at least ~3 km thick, with only a very tentative upper bound at 3-4 km thick. This stratigraphy supports the presence of a darkening agent at depth outside Caloris in quantities sufficient to darken a layer of LRM at least 3 km in thickness (8+ km if the quantity in Caloris is typical), consistent with the hypothesis of a buried primary crust. On the basis of these two data points for darkening agent quantity, we speculate on what this might mean for the nature of the primary crust.

If the LRM is darkened by 2-6 wt.% graphite [11, 12, 13] originating from carbon dissolved in the magma ocean, and if the quantities darkening the LRM layers interior to Rembrandt and Caloris are typical of the global stratigraphic column, we calculate that Mercury's magma ocean must have contained at least 130 ppm (3 km thick LRM, 2 wt.% graphite) to 1030 ppm (8 km thick LRM, 6 wt.% graphite) carbon. This is almost certainly a lower bound, since both Rembrandt and Caloris excavate LRM, and additional darkening agent may remain in the deep crust below one or both basins. While 130-1030 ppm does overlap with the high end of the plausible range of carbon solubility in silicate melt under reducing conditions (e.g., 11-192 ppm [14]) such concentrations require either >3 wt.% bulk carbon, more than major chondrite groups [3] or a carbon metal-silicate partitioning coefficient < 300, lower than usually found experimentally (e.g., 180-4600 [14]), even in low-C systems (~1800 for Mercury [15]).

This suggests that an alternate source of carbon should be considered. Within the flotation crust paradigm, carbon present in excess of planetary saturation in Mercury's early history could have contributed to the primary crust. Alternatively, if carbon should be expected to continuously float as graphite during accretion rather than equilibrate between the core and mantle [16], the graphite in the layer exposed as LRM might represent Mercury's total carbon content.

Summary and future work: Exposures of LRM in Rembrandt basin are consistent with a layer at depth at least ~3 km thick, potentially corresponding to the basin interior melt sheet. This aligns with the results of [4] for Caloris basin and adds to the body of evidence supporting the presence of a darkening agent at depth outside Caloris. LRM layer thickness in these two basins combined with estimates of carbon content of LRM suggest either 1) a surprisingly high magma ocean C concentration (given expected silicate melt C solubility and metal-silicate partitioning), or 2) an alternate source of graphite. Work is underway to extend this detailed analysis to basins beyond the Caloris-Rembrandt pair to further constrain the LRM quantity and distribution in the crust. This new information and higher spatial and spectral resolution data from the ESA BepiColombo mission promise to give insight into Mercury's early evolution.

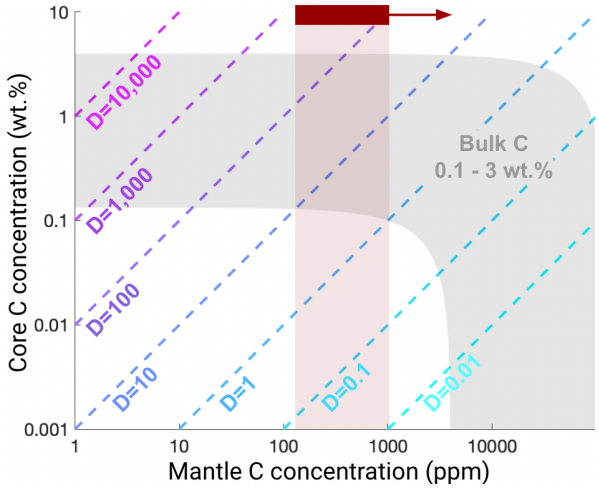

Figure 2. Relationships between core and mantle carbon concentration, bulk carbon, and partition coefficient. Diagonal dashed lines indicate C concentrations corresponding to a particular metal-silicate partition coefficient (D). The grey shaded region represents bulk C concentrations of 0.1-3 wt.%, rough bounds on chondritic carbon abundance [3]. The red region indicates the estimated lower bound on C abundance in the magma ocean (130-1030 ppm) derived from estimates of LRM layer thickness as exposed by Rembrandt and Caloris combined with measurements of C content of LRM. A magma ocean C concentration in the red range requires either D < 300 or bulk C > 3 wt.%.

References: [1] Hiesinger, H. and Head, J. W. (2006) *Rev. in Min. and Geochem., 60(1),* 1-81. [2] Shearer C. K. et al. (2006) *Rev. in Min. and Geochem., 60(1),* 365-518. [3] Vander Kaaden K. E. and McCubbin F. M. (2015) *JGR, 120(2)*, 195-209. [4] Ernst C. M. et al. (2015) *Icarus, 250,* 413-429. [5] Watters T. R et al. (2009) *Science, 324(5927),* 618-621. [6] Whitten J. L. and Head J. W. (2015) *Icarus, 258,* 350-365. [7] Semenzato A. M. et al. (2020) *Remote sensing, 12(10),* 3213. [8] Hall, G. P. et al. (2021) *JGR: Planets, 126(9),* e2021JE006839. [9] Kinczyk, M. J. et al. (2020) *Icarus, 341,* 113637. [10] Hawkins S. E. et al. (2007) *Space Science Rev., 131(1),* 247-338. [11] Murchie S. L. (2015) *Icarus, 254,* 287-305. [12] Peplowski, P. N. et al. (2016) *Nature Geosc., 9(4),* 273-276. [13] Klima R. L. (2018) *GRL, 45(7),* 2945-2953. [14] Li, Y. et al. (2017) *JGR: Planets, 122,* 1300-1320. [15] Grewal D. S. et al. (2021) *EPSL, 571,* 117090. [16] Keppler H. and Golabek G. (2019), *Geochem. Perspect. Lett, 11,* 12-17.